Chapter

Vibration Analysis and Control in the Rail Car System Using PID Controls

Ilesanmi Afolabi Daniyan and Khumbulani Mpofu

Abstract

The PID classic control systems are often employed for rail car systems to reduce the vibrations and disturbance rate during movement. In this study, the dynamic modeling and simulation of PID controls for rail car systems were carried out. Using 9 degrees of freedom, the modeling process comprises the representation of the rail car system and the rail track followed by the generation of equations of motion as well as differential equations for the rail car body, wheel sets and bogie. The represented systems are simulated in the MATLAB Simulink 2018 environment based on the equations of motion generated, and subsequently vibration analysis was carried out. The PID control system tuned according to the Nichols-Ziegler rule was introduced to minimize the vibrations and disturbance rate. The performance of the control and the rail car system in terms of the input step response, bandwidth, frequency, phase margin, frequency and input and output rejections was evaluated. The control system demonstrated significant robustness in providing the required active control for the system, while there was improved stability and reduction in noise and vibration under control action of the PID, thus improving ride comfort.

Keywords: advanced controls, modeling, rail car, simulation, vibration

1. Introduction

The rail car system uses steel wheels moving on steel rails, and its suspension system comprises the bogie, primary and secondary suspension elements as well as springs and dampers. The rail car has the power bogies in the front and rear positions each having four wheels arranged in pairs and rigidly connected through an axle. The sets of wheel, which rotates at the same speed, are connected to the bogie through the primary suspension system, which is harder and stiffer in order to minimize load disturbances and uneven weight distributions. This is to maintain a good balance of the rail car while moving along its track. The stiff primary suspension system connects the wheel set to the bogie, while the soft secondary suspension system connects the bogie to the rail car body in order to isolate it from disturbances that stem from rail irregularities, uneven track profiles and its associated vibrations. While the primary suspension system is designed to provide guidance and rail car stability amidst load and weight variations, the secondary suspension system is to enhance comfortable ride by isolating rail car body from rail

track irregularities. These design requirements of both suspension systems are to dampen the effect of vibration and increase the overall system's performance [1, 2]. For a rail car, when vibrations are not kept within the permissible limits, the comfort, safety and health of passengers are at risk, and the time interval for maintenance activities for the components will likely increase. Hence, undesirable vibration in the rail car system is the cause of noise, considerable energy loss, reduction in the system's performance, fatigue or fracture of some component, instability of a moving rail car and displacement of the rail track, amongst others. Over the years, there are three main types of suspension systems often employed to check vibration in the rail car system, namely, the passive, semi-active and fully active suspension systems [3, 4]. The design requirements of the suspension system of the rail car are to provide support against the dynamic loads and weight of the railcar; prevent load and rail disturbances; isolate the rail car body disturbances that could offset its balance; prevent irregular motions such as bouncing, yawing, etc.; provide guidance along the rail track; and optimize the curving, braking and other car maneuvering performances. The passive suspension system, which consists of springs, absorbs and stores the energy absorbed, while the dampers mounted on each wheel act as the shock absorber that dissipates the energy stored in the spring and reduces the vibrations from the rail transmitted to the vehicle ([5–7]. The passive suspension system is cost-effective and driven by simple technology, but its demerit lies in the fact that it cannot measure some critical parameters such as the velocity, displacement, acceleration, etc. of the rail car system in real time in order to effect the needed adjustments to stabilize the rail car system; hence, it is rigid and cannot reach the compromise between alternate hard primary and soft secondary suspension systems amidst load and rail irregularities. On the other hand, the active suspension system uses sensors, comparators and actuator for measuring and monitoring some critical parameters that influence rail car stability in real time [8, 9]. The measured system's parameters are compared with the threshold already pre-set on the controller, which can guarantee comfortable ride. The steady-state errors generated are eliminated through adjustment and compensation for such errors, and as such, there is high-level damping without compromising the system's performance. The third category of suspension system is the semi-active suspension system, which employs a spring and controllable damper. The spring element stores the energy, while the controllable damper dissipates the energy stored. The semi-active suspension systems combine the features of the passive and active suspension systems such as the use of passive damper and an actively controlled spring. The merit of the semi-active suspension is that it is cost and energy effective [9–11].

Over the years, researchers have employed several approaches ranging from classic to advance systems to control the suspension system in order to minimize the effect of vibrations. Such approaches include the use of proportional-integral-derivative (PID) control, Fuzzy PID, Linear Quadratic Regulator vibration controller, Adaptive Neuro-Fuzzy Inference System control and magnetorheological dampers, amongst others [12–16].

2. Materials and method

The analysis of vibration and control in the rail car system starts with the schematic representation of the rail car and track system including their degrees of freedoms and subsequent generation of equations of motion. The modeling is done with the masses of the system (rail car, body and wheel sets) having 6 degrees of freedom in the longitudinal, lateral and vertical directions as well as in the roll, pitch

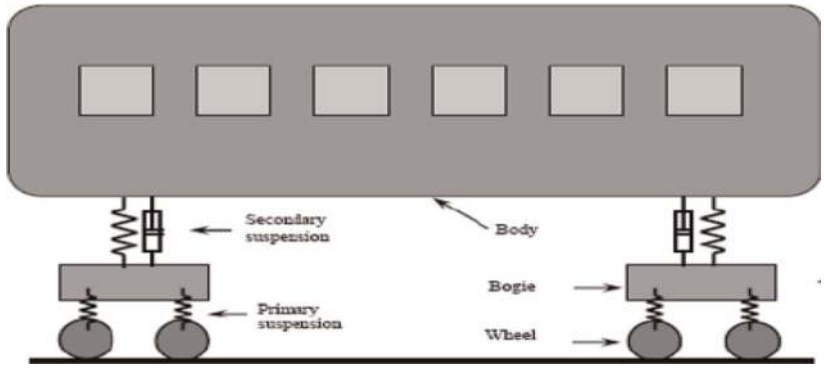

Figure 1.
The rail car and its suspension system [17].

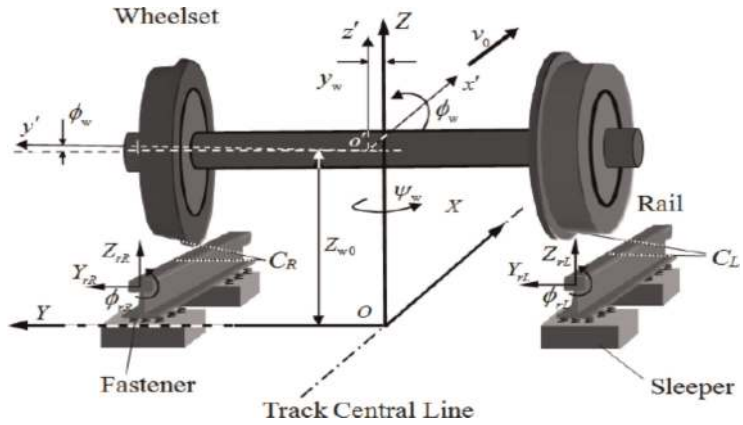

Figure 2.
The free body diagram for the rail car model [18].

and yaw rotational motions. **Figures 1** and **2** illustrate the free body diagram for the rail car and track system in their degrees of freedom.

In order to give a complete vibration analysis and control, the model design and simulation of the suspension systems are considered as both linear and non-linear systems. There are three forces acting on the rail car suspension system, namely, the spring force, rolling resistance and forces due to the wheel-track interactions. The spring force and the rolling resistance act on the rail car body with mass m_1 in the horizontal directions, while the spring force, rolling resistance and the forces due to the wheel-track interactions act on the bogies with mass m_2 due to load in the horizontal directions. The masses of the rail car and its bogies are represented by m_1 and m_2, respectively, while the bodies are connected to the rail car through the secondary suspension with couplings having stiffness K. If force F_d is the force generated as a result of wheel-track interaction, F_u is the control force and μ is the coefficient of rolling friction, then Newton's second law of motion holds; thus,

$$F = ma \tag{1}$$

$$\sum F_1 = K(x_1 - x_2) - \mu m_1 g\dot{x}_1 = m_1\ddot{x}_1 \tag{2}$$

$$\sum F_2 = F_d - K(x_1 - x_2) - \mu m_2 g\dot{x}_2 = m_2\ddot{x}_2 \tag{3}$$

Eq. (3) expresses the summation of the forces

$$\sum (F_1 + F_2) = m_1\ddot{x}_1 + m_2\ddot{x}_2 \tag{4}$$

$$\sum(F_1 + F_2) = M\ddot{x} \tag{5}$$

$$\sum(F_1 + F_2) = \sum(F_d + F_u) \tag{6}$$

The spring deflection is expressed as Eq. (7):

$$\delta = K(x_1 - x_2) \tag{7}$$

$$\sum(F_d + F_u) = M\ddot{x} + b\dot{x} + Kx \tag{8}$$

$$[F_d] + [F_u] = [M]\ddot{x} + [b]\dot{x} + [K]x \tag{9}$$

$$\text{Hence, } x = \left[x.....x^1\right]^T \tag{10}$$

$$\dot{x} = \frac{dx}{dt} = f(x(t), u(t), t) \tag{11}$$

where $x(t)$ is the state vector and a set of variables representing the configurations of the system. The modeling of the rail car system and its suspension system as well as the track system is done on the MATLAB Simulink 2018 environment (**Figure 3**).

The transfer function was used for representing the linear systems, and the inputs are the load changes, applied forces as well as the uneven track profiles, while the output of the system is the acceleration and displacement of the rail car body as well as the deflection of the suspension systems.

According to Sezer and Atalay [19], the vectors for the displacement, rail car disturbance and control forces are expressed as Eqs. (12)–(14), respectively:

$$\begin{aligned} \mathrm{x} = \big[&\mathrm{X_r}, \mathrm{L_r}, \mathrm{V_r}, \theta_\mathrm{r}, \varnothing_\mathrm{r}, \psi_\mathrm{r}, \mathrm{X_{b1}}, \mathrm{L_{b1}}, \mathrm{V_{b1}}, \theta_{\mathrm{b1}}\varnothing_{\mathrm{b1}}, \psi_{\mathrm{b1}}, \mathrm{X_{b2}}, \mathrm{L_{b2}}, \mathrm{V_{b2}}, \theta_{\mathrm{b2}}\varnothing_{\mathrm{b2}}, \psi_{\mathrm{b2}}, \\ &\mathrm{X_{b3}}, \mathrm{L_{b3}}, \mathrm{V_{b3}}, \theta_{\mathrm{b3}}\varnothing_{\mathrm{b3}}, \psi_{\mathrm{b3}}, \mathrm{X_{w1}}, \mathrm{L_{w1}}, \mathrm{V_{w1}}, \theta_{\mathrm{w1}}, \psi_{\mathrm{w1}}, \mathrm{X_{w2}}, \mathrm{L_{w2}}, \mathrm{V_{w2}}, \theta_{\mathrm{w2}}, \\ &\psi_{\mathrm{w2}}, \mathrm{X_{w3}}, \mathrm{L_{w3}}, \mathrm{V_{w3}}, \theta_{\mathrm{w3}}, \psi_{\mathrm{w3}}, \mathrm{X_{w4}}, \mathrm{L_{w4}}, \mathrm{V_{w4}}, \theta_{\mathrm{w4}}, \psi_{\mathrm{w4}}, \mathrm{X_{w5}}, \mathrm{L_{w5}}, \mathrm{V_{w5}}, \\ &\theta_{w5}, \psi_{w5}, X_{w6}, L_{w6}, V_{w6}, \theta_{w6}, \psi_{w6}]T \end{aligned} \tag{12}$$

$$\begin{aligned} [F_d] = [&0000000000000000000000(k_{sL}Y_{r1})(k_{sV}(V_{r1} + V_{r2})) \\ &(k_{sL}R_1L_{r1} + k_{sV}(V_{r2} - V_{r1}))00(k_{sL}L_{r2})(k_{sV}(V_{r3} + V_{r4})) \\ &(k_{sL}R_1L_{r2} + k_{sV}a(V_{r4} - V_{r3}))00(k_{sL}L_{r3})(k_{sV}(V_{r5} + V_{r6})) \\ &(k_{sL}R_1L_{r3} + k_{sV}a(V_{r6} - V_{r5}))00\ (k_{sL}L_{r4})(k_{sV}(V_{r7} + V_{r8})) \\ &(k_{sL}R_1L_{r4} + k_{sV}a(V_{r8} - V_{r7}))00\ (k_{sL}L_{r5})(k_{sV}(V_{r9} + V_{r10})) \\ &(k_{sL}R_1L_{r5} + k_{sV}a(V_{r10} - V_{r9}))00(k_{sL}L_{r6})(k_{sV}(V_{r11} + V_{r12})) \\ &(k_{sL}R_1L_{r6} + k_{sV}a(V_{r12} - V_{r11}))0]^T \end{aligned} \tag{13}$$

$$\begin{aligned} [\mathrm{F_u}] = [&0(\mathrm{U_{L1}} + \mathrm{U_{L2}} + \mathrm{U_{L3}})(\mathrm{U_{V1}} + \mathrm{U_{V2}} + \mathrm{U_{V3}} + \mathrm{U_{V4}} + \mathrm{U_{V5}} + \mathrm{U_{V6}}) \\ &\left(\mathrm{d_3}(\mathrm{U_{L1}} + \mathrm{U_{L2}} + \mathrm{U_{L3}})\left(p_2((U_{V2} + U_{V4} + U_{V6}) - (U_{V1} + U_{V3} + U_{V5}))\right)\right. \\ &L_o((U_{V5} + U_{V6}) - (U_{V1} + U_{V2})))(h_2U_{L1} - U_{L3}))0 \\ &-(U_{L1})((U_{V1} + U_{V2}))\left(d_2U_{L1} - p_2(U_{V2} - U_{V1})\right)000(-U_{L2}) \\ &(-U_{V3} + U_{V4}))\left(d_2U_{L2} - p_2(U_{V4} - U_{V3})\right)000(-U_{L3})(-U_{V5} + U_{V6})) \\ &\left(d_2U_{L3} - p_2(U_{V6} - U_{V5})\right)0000000000000000000000000000000]^T \end{aligned} \tag{14}$$

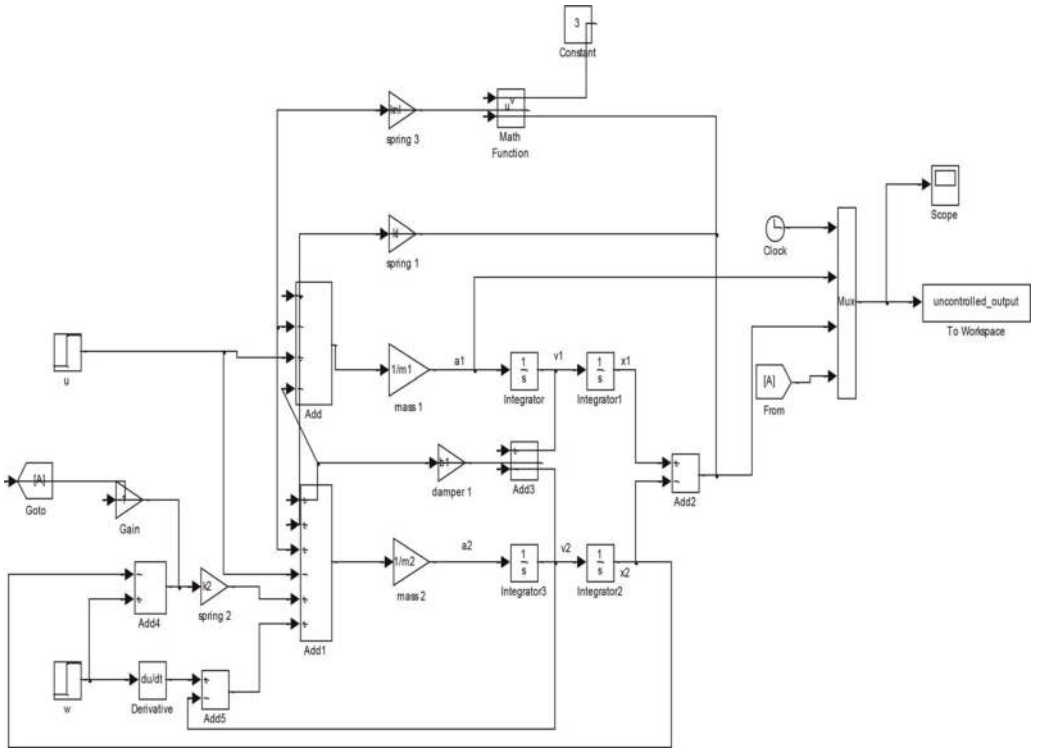

Figure 3.
Modeling of the rail car and its suspension system.

where.

$L_{r1}, L_{r2}, L_{r3}, L_{r4}, L_{r5}, L_{r6}$ are the lateral rail disturbance functions; $V_{r1}, V_{r3}, V_{r5}, V_{r7}, V_{r9}, V_{r11}$ are the vertical right rail disturbance functions; $V_{r2}, V_{r4}, V_{r6}, V_{r8}, V_{r10}, V_{r12}$ are the vertical left rail disturbance functions; X_r, L_r, V_r are the longitudinal, lateral and vertical displacements of the rail car body; X_{bi}, L_{bi}, V_{bi} are the longitudinal, lateral and vertical displacements of the rail car bogie; X_{wj}, L_{wj}, V_{wj} are the longitudinal, lateral and vertical displacements of the rail car wheel sets; $\theta_r, \varnothing_r, \psi_{r,}$ are the roll, pitch and yaw displacements of the rail car body; $\theta_{bi}, \varnothing_{bi}, \psi_{bi,}$ are the roll, pitch and yaw displacements of the rail car bogie; $\theta_{wj}, \varnothing_{wj,}\ \psi_{wj,}$ are the roll, pitch and yaw displacements of the rail car wheel set $(i = 1.....3; and\ j = 1.....6)$; p_1 is the lateral distance between the vertical primary suspensions; p_2 is the lateral distance between the vertical secondary suspensions; d_1 is the vertical distance between the wheel set and the bogie mass centre; d_2 is the vertical distance between the bogie mass centre and lateral secondary suspension; d_3 is the vertical distance between the lateral secondary suspension and railcar body mass centre; L_o is the longitudinal distance between the bogies; and a is the lateral distance between the contact points of the wheel-rail.

The mathematical model can be obtained in either the state space or using the transfer function for necessary control actions. The control action is to improve the speed of response, system's balance and stability and to reduce the steady-state error as well as the amplitude of oscillations. Eqs. (15) and (16) express the form of the second-order systems:

$$\dot{y}(t) + \xi\omega_n\dot{y}(t) + \omega_n^2 y(t) = k_d\omega_n^2 u(t) \tag{15}$$

$$G(s) = \frac{X(s)}{F(s)} = \frac{1}{ms^2 + bs + k} = \frac{k_d\omega_n^2}{s^2 + 2\xi\omega_n s + \omega_n^2} = \frac{k_d\omega_n^2}{(s+\sigma)^2 + \omega_d^2} \tag{16}$$

where.

k_d is the dc gain which is the steady-state step response to the magnitude of the step input expressed as Eq. (17)

$$k_d = \frac{1}{k} \tag{17}$$

ω_d is the damped natural frequency expressed as Eq. (18)

$$\omega_d = \omega_n \sqrt{1 - \xi^2} \tag{18}$$

σ is the real part of the pole expressed as Eq. (19)

$$\sigma = \xi \omega_n \tag{19}$$

ω_n is the undamped natural frequency at which the system oscillates expressed as Eq. (20)

$$\omega_n = \sqrt{\frac{k}{m}} \tag{20}$$

ξ is the damping ratio which defines the rate or nature of amplitude of oscillation (Eq. (21))

$$\xi = \frac{b}{2\sqrt{km}} \tag{21}$$

The performance of the control system is measured by the settling time, delay time rise time, percent overshoot and the steady-state error.

The settling time t_s is the time it takes the system to fall within a certain percent (mostly 2%) of the steady-state value for a step input response expressed as Eq. (22):

$$t_s = \frac{-lnT_f}{\xi \omega_n} = 4\zeta = \frac{4}{\sigma} \tag{22}$$

On the other hand, the rise time is the time it takes the signal to change from a low value to a high value (say 10–90% or 0–100%). The time it takes the peak value to occur known as the time is expressed as Eq. (23):

$$t_p = \frac{\pi}{\omega_d} \tag{23}$$

The steady-state error $E(s)$ is the difference between the input reference signal $R(s)$ and the output signal $Y(s)$ expressed as Eq. (24):

$$E(s) = R(s) - Y(s) \tag{24}$$

Similarly, the delay time is the time required for the response to reach half the final value for the first time, while the percent overshoot is the percent by which the step response of the system exceeds the final steady-state value. It is a parameter that defines the instability of a system (Eq. (25)):

$$P_o = e^{-1}\frac{\zeta\pi}{\sqrt{1-\xi^2}} \tag{25}$$

Eq. (26) relates the percent overshoot to the damping ratio:

$$\xi = \frac{-lnP_o}{\sqrt{\pi^2 + ln^2(P_o)}} \tag{26}$$

The input parameters of the system are presented in **Table 1**.

2.1 The proportional-integral-derivative (PID) control

The PID control represents the proportional, integral and derivative controls. It is a form of classic control designed to automatically reduce rise and settling times, steady-state errors and percent overshoot. The block diagram of the PID controller is illustrated in **Figure 4**. The threshold value otherwise referred to as the reference point is pre-set on the controller while real-time measurement using sensors is taken. The error generated, which is the difference between the threshold value and the actual measurement, represents the deviation from the ideal process; thereafter, the actuator effects real-time control to adjust process variables. The output signal of the PID controllers often responds to changes over time with respect to the actual

S/N	Parameter	Notation	Value	Unit
1	Average mass of the rail car	M_1	50,500	kg
2	Average mass of bogie	M_2	2410	kg
3	Mass of primary suspension system	M_p	30,000	kg
4	Mass of secondary suspension system	M_s	30,000	kg
5	Moments of inertia	I_i	56,900	kgm^2
6	Rail car roll inertia	I_r	68,200	kgm^2
7	Rail car pitch inertia	I_p	71,000	kgm^2
8	Average mass of first wheel set and axle	m_1	1300	kg
9	Average mass of second wheel	m_2	1300	kg
10	Distance between the centre of gravity and the front position of the rail car	d_i	6	m
11	Distance between the centre of gravity and the middle position of the rail car	d_2	6	m
12	Distance between the centre of gravity and the rear position of the rail car	d_3	6	m
13	Spring constant of the primary suspension system	k_1	2.4×10^6	N/m
14	Spring constant of the secondary suspension system	k_2	5.6×10^5	N/m
15	Spring constant of the wheel	k_3	4.0×10^5	N/m
16	Damping constant of the primary suspension system	b_1	1.2×10^3	Ns/m
17	Damping constant of the secondary suspension system	b_2	2.95×10^4	Ns/m
18	Damping constant of the wheel	b_3	5.0×10^4	Ns/m

Source: [20, 21].

Table 1.
Input parameter for rail car system modeling.

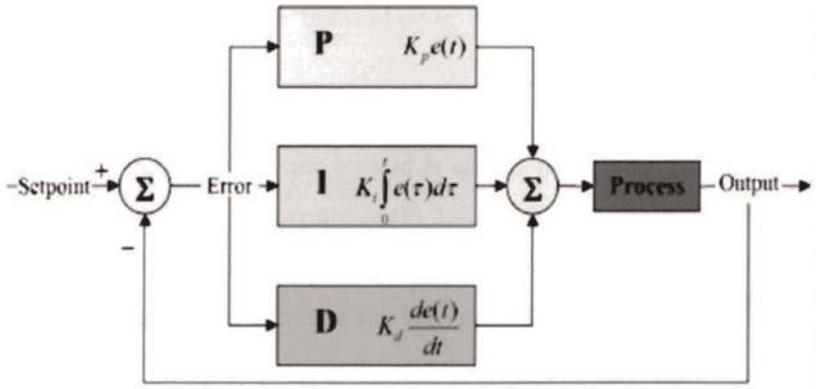

Figure 4.
The block diagram of the PID controller.

measurements and set points. The PID variables are iteratively adjusted until the steady-state error from the output signal is eliminated. This control action is done by adjusting the controller gain with resulting decrease in the rise time and percent increase in the overshoot, which makes the system go unstable. This rise time is further reduced with the integral control action. Finally, the derivative action is introduced to compensate for the offset. This reduces the percent overshoot and settling time, thus making the system stable over time.

Eq. (27) gives the expression for the control action of the PID controller:

$$u_c = K_p e(t) + \frac{K_i}{T_i}\int_0^t e(t)dt + K_d T_d \frac{de(t)}{dt} \tag{27}$$

The Nichols-Ziegler tuning rules employed for tuning the PID control as well as the summary of the effects of its control action on the PID are presented in **Tables 2** and **3**, respectively.

The signal (U) which passes through the controller computes the derivative and integral of error signal. The signal error is thereafter sent to the system in order to obtain the system's output (Y). The PID controller was designed in the MATLAB Simulink 2018 environment to generate a continuous time control. Using the Nichols-Ziegler rules, the tuning of PID controller was done by generating the

S/N	Type of controller	K_p	K_i	K_d
1	P	0.5 Kcr	∞	0
2	PI	0.45 Kcr	0.83 Pcr	0
3	PID	0.6 Kcr	0.5 Pcr	0.125 Pcr

Table 2.
Zeigler-Nichols tuning rules.

S/N	Controller response	Rise time	Overshoot	Setting time
1	K_p	Decrease	Increase	Small change
2	K_i	Decrease	Increase	Increase
3	K_d	Small change	Decrease	Decrease

Table 3.
Effect of the control action of the PID.

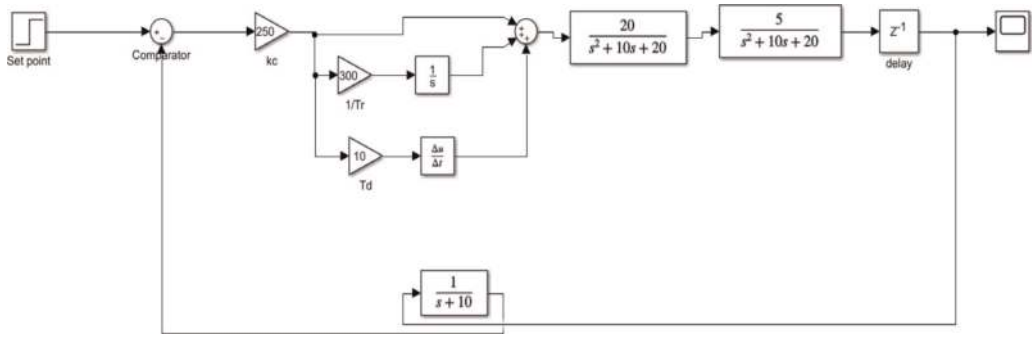

Figure 5.
The PID control system.

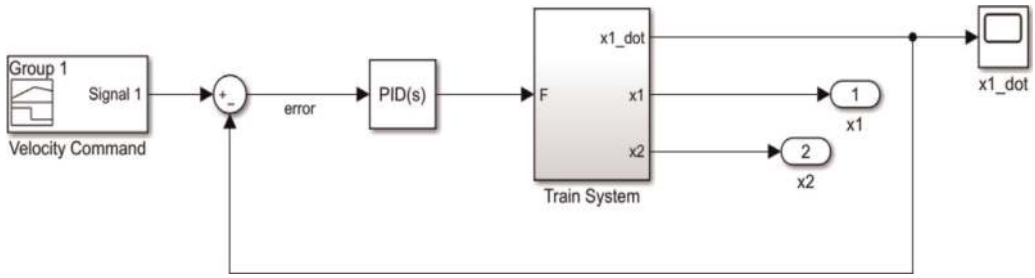

Figure 6.
The PID control and the rail car systems.

system's transfer function and subsequent importation of the parameters obtained into the linear time-invariant system.

The PID control system and its connection to the rail car system are shown in **Figures 5** and **6**, respectively.

The aim of the control design is to keep the system variables close to the reference in order to compensate for the effect of load and rail disturbances. The system requirement is to check unpleasant motion and ensure rail car stability by reaching a compromise between the stiff primary suspension and soft secondary suspension system.

The actively controlled suspension system can be activated via the use of solenoid, hydraulic, electromagnetic means or through a magnetorheological damper. This system is designed to use the solenoid actuators because of its lightweight, simplicity in structure, ease of installation and short response time, which makes it highly sensitive to disturbances.

3. Results and discussion

Figure 7 shows the step response before the iterative adjustment of the PID control. The amplitude of oscillation, which is a function of the percent overshoot, is 2 mm, and the system could not return to the equilibrium position after 3 s. The shape of the plot represents a system that is underdamped, which signifies the need for damping to minimize unwanted motion. The system whose step response is depicted in **Figure 7** is relatively unstable as vibration will reduce the system's and ride performance.

Figure 8 shows the step response from the controlled system. When compared to **Figure 1**, the amplitude of oscillation has reduced to 1.15 mm and settling time 0.5 s under the effect of the PID control action. The system is relatively stable as the

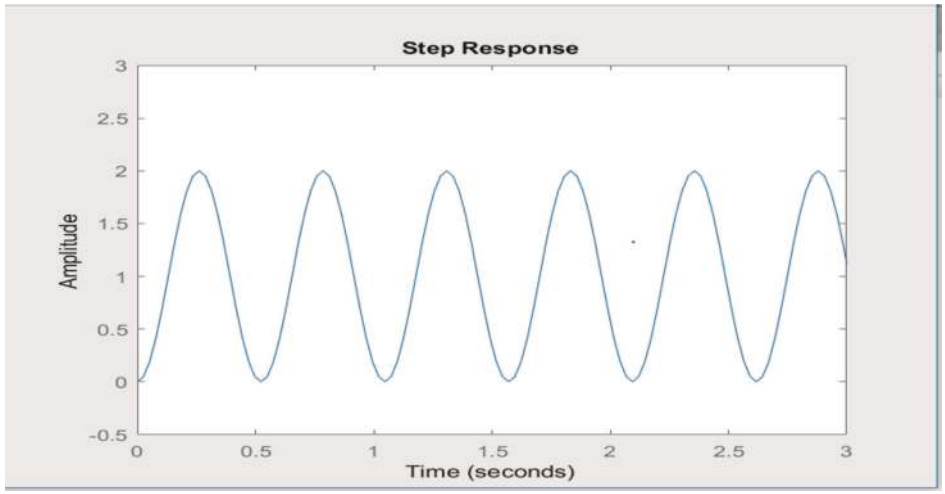

Figure 7.
Step response for the uncontrolled system.

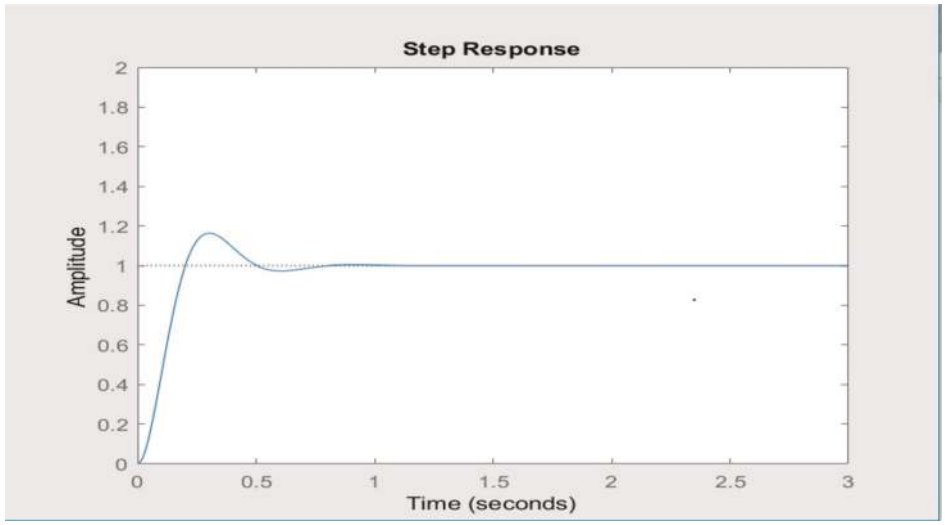

Figure 8.
Step response for the controlled system.

plot gives an indication of a critically damped system. This implies that under the effect of the PID control system, the system could regain its stability and equilibrium position after encountering some level of disturbances.

Figure 9 shows the response of the PID controller in order to determine whether the control system meets the design requirements. The tuned response represents the actual measurement of the process variables, while the baseline response represents the reference or set point. The differences between the tuned response and the baseline response give the steady-state error. The nature of the plot also indicates that the system is critically damped; thus, the damping ratio $\xi = 1$.

Figure 9 shows the reference tracking of the tuned response and the reference (baseline). The design requirement of the control system includes set-point tracking; hence, this plot shows how the closed-loop system responds to a step change in set point. From the plot, the steady-state error is minimal, thus indicating the effectiveness of the control system.

Figure 10 shows the closed-loop step response to a step disturbance at the system's output. This is important in analyzing the sensitivity of the control system

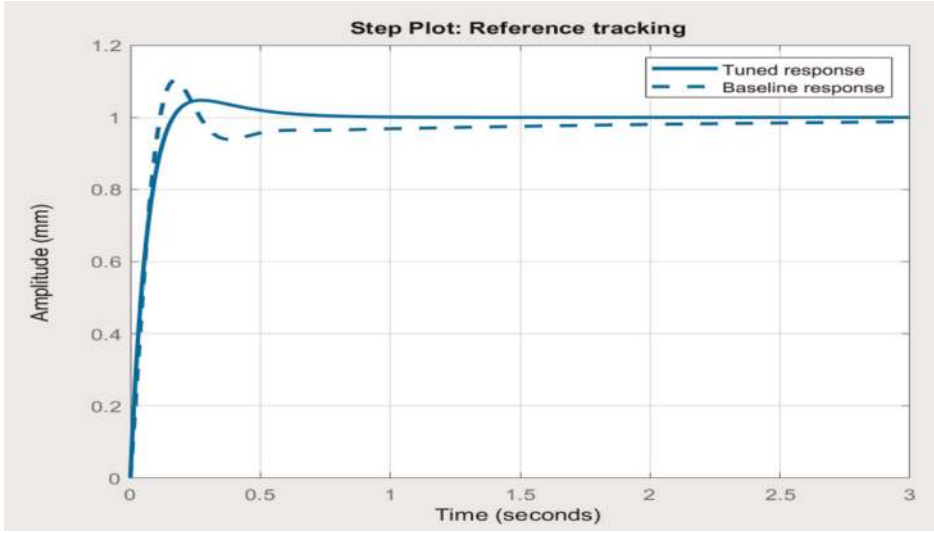

Figure 9.
Step plot for reference tracking.

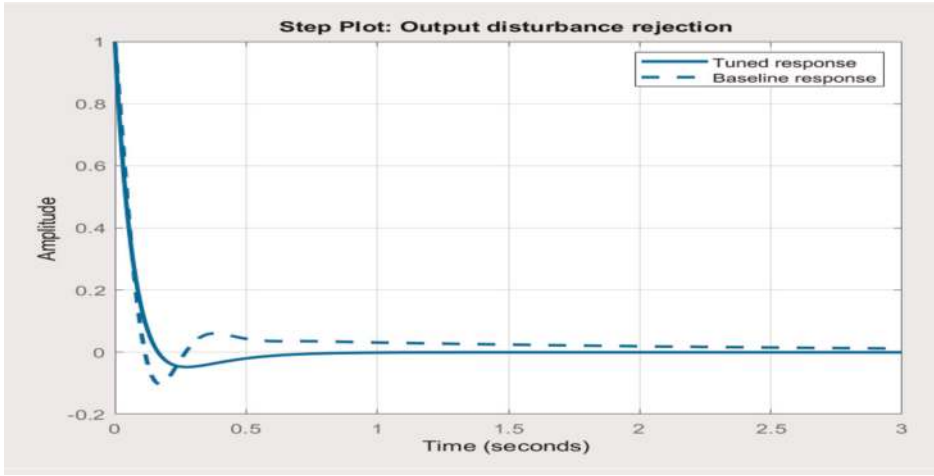

Figure 10.
Plot of output disturbance rejection.

to noise measurement. The negligible value of the steady-state error as shown by the degree of agreement between the tuned output response of the system and the baseline (reference) indicates the high sensitivity and compensation of the system's control to the noise measurement.

Figure 11 shows the closed-loop system response to load disturbance. The plot represents a step disturbance from the system's input. The differences between the tuned response and the baseline response, which is a function of the steady-state error, are significantly large. The implication of this is that the control system is insensitive to the rejection of load and other input disturbances, which is capable of offsetting the balance of the system. The large steady-state error resulting from input disturbance rejection stems from the fact that a single PID may not be able to satisfy all the design requirements at the same time; hence, there is always a performance trade-off amongst the reference tracking, percent overshoot and input disturbance rejection. However, the use of Fuzzy PID or ISA-PID controller can be used to meet the design requirements significantly. This will improve the response of the reference tracking with the provision of an additional tuning parameter,

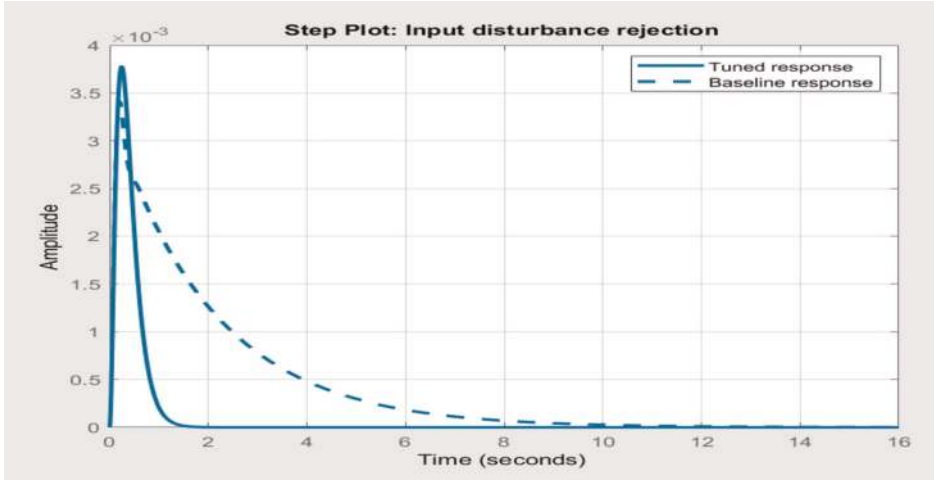

Figure 11.
Plot of input disturbance rejection.

Parameter	Tuned response	Baseline (reference) response
Rise time	0.07 s	0.0847 s
Settling time	0.499	1.94 s
Overshoot	4.76%	10.3%
Peak	1.05	1.1 mm
Phase margin	83°	60.4°
Frequency	16.6	17.8 rad
Closed loop	Stable	Stable

Table 4.
Summary of the performance of the PID control.

which allows for independent control of the effect of the reference signal on the proportional action.

The robustness and performance of the PID control are directly proportional to the degree of stability of the rail car, ride comfort and performance of the rail car. The summary of the performance of the PID control system is presented in **Table 4**.

From **Table 4**, the tuned response has better performance and robustness compared to the baseline due to periodic iterative adjustment to eliminate the steady-state error for each step input. The rise time of the tuned response indicates a fast response time of the control system to disturbances or changes when compared to the baseline. This signifies some degree of delay in the time it takes the system to respond to fluctuations. In addition, comparing the settling time for both responses, the tune response settles faster after some disturbances compared to the baseline response. This explains the ability of the rail car to regain its stability after encountering some level of disturbances with the active control system. Also, the percent overshoot for the tuned response is still within the range of the permissible oscillation (5%) for critically damped system which indicates that the rail car system is relatively stable amidst load and rail disturbances. An increase in the phase margins implies a significant reduction in the percent overshoot and bandwidth.

Figure 12 shows the bode response of the control system. This is the plot of the frequency and phase response of the control system. The phase margin was found to

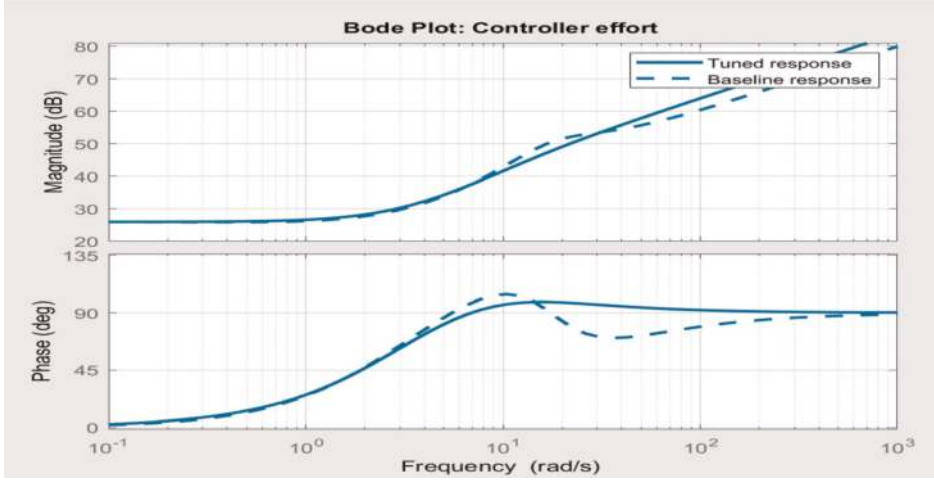

Figure 12.
Bode plot for the controller effort.

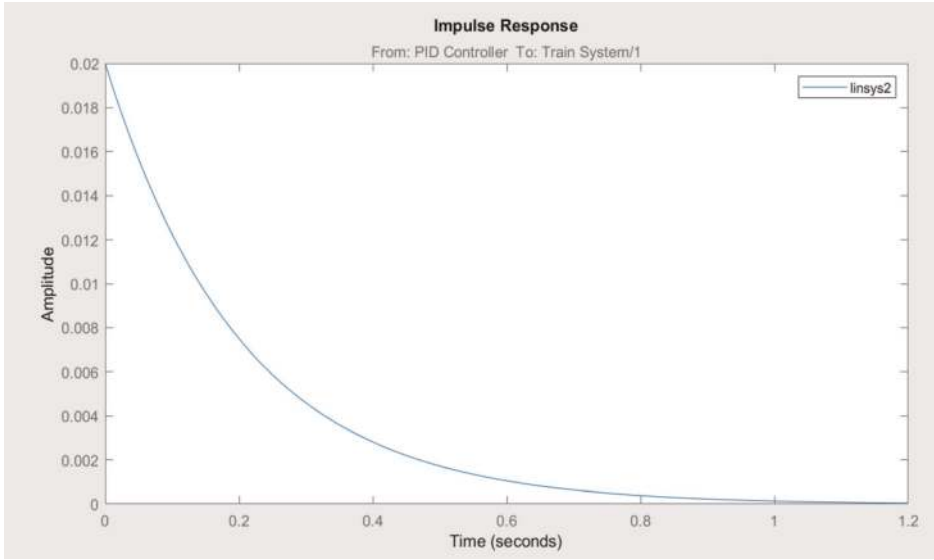

Figure 13.
Impulse response of the actively controlled rail car.

be 83° at a frequency of 16.6 rad/s for the tuned response compared to the baseline response with a phase margin and frequency of 60.4° and 17.8 rad/s, respectively. The relationship between the phase margin and percent overshoot is inversely proportional. Hence, the high value of the phase margin results in significant decrease in the percent overshoot, thus improving the rail car stability. Also, the higher closed-loop bandwidth results in faster rise time. The rise time was found to be 0.07 s for the tuned response and 0.0847 s for the baseline response. This implies that for the baseline response, the percent overshoot is still significant to offset the stability of the rail car system.

Figures 13 and **14** show the result of the linearization of the rail car system. This is to determine the dynamics of the system in real time and within time and frequency domains. **Figure 13** shows the impulse response of the rail car system, which is the degree of rail car body displacement as a result of load or rail disturbances. The maximum amplitude oscillation is 0.02 mm, which is negligible and insufficient to offset the rail car balance. In addition, the settling time (less than 1 s)

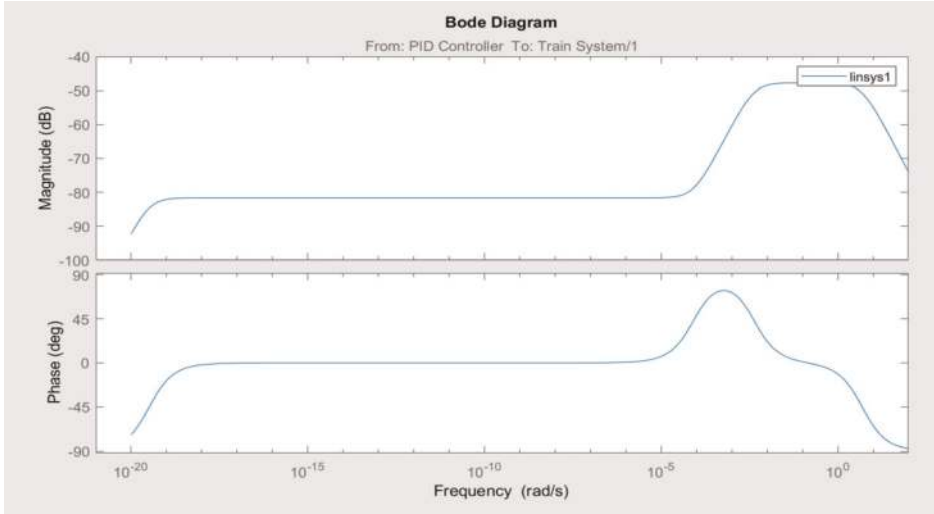

Figure 14.
Bode plot for the actively controlled rail car.

is also within the permissible range indicating the ability of the system to regain its stability within a second as a result of load or rail disturbances.

Figure 14 shows the bode plot of the rail car system; the phase margin was found to be 48° at a frequency of 20.2 rad/s which signifies significant reduction in the percent overshoot due to the compensation for steady-state error by the derivative action of the PID.

4. Conclusion

The control of undesirable vibrations of the rail car system in 6 degrees of freedom was carried out using the PID control system. The initial displacement and vertical acceleration that characterize the performance of the system on encountering rail and load disturbances were minimized with the iterative adjustment of the PID controller according to Nichols-Ziegler tuning rules. In addition, the performance of the control and the rail car system in terms of the input step response, bandwidth, frequency, phase margin and input and output rejections was within the acceptable range. Hence, the PID control system shows significant robustness in providing the required active control for the system, while the rail car system shows improved stability and reduction in vibration under control action of the PID, thus improving ride comfort. However, a single PID may not sufficiently satisfy all the design requirements at the same time resulting in performance trade-off. However, Fuzzy PID or ISA-PID controller can be used to meet the design requirements significantly. This will further improve the performance and robustness of the rail car system.

Author details

Ilesanmi Afolabi Daniyan* and Khumbulani Mpofu
Department of Industrial Engineering, Tshwane University of Technology, Pretoria, South Africa

*Address all correspondence to: afolabiilesanmi@yahoo.com

References

[1] Al-Zughaibi A, Davies H. Controller design for active suspension system of quarter car with unknown mass and time-delay. International Journal of Mechanical, Aerospace, Industrial, Mechatronic and Manufacturing Engineering. 2015;**9**(8):1484-1489

[2] Sharma RC, Sharma SK. Sensitivity analysis of three-wheel vehicle's suspension parameters influencing ride behaviour. Noise & Vibration Worldwide. 2018;**49**(7–8):272-280

[3] Bideleh SMM, Mei TX, Berbyuk V. Robust control and actuator dynamics compensation for railway vehicles. Vehicle System Dynamics. 2016;**54**(12): 1762-1784

[4] Yao JL, Shi WK. Development of a sliding mode controller for semi-active vehicle suspensions. Journal of Vibration and Control. 2013;**19**: 1152-1160

[5] Arefsoliman MA. Adaptive LQR control strategy for active suspension system. 2011. SAE Technical Paper, 2011-01-0430

[6] Herbst G. A simulative study on active disturbance rejection control (ADRC) as a control tool for practitioners. Electronics. 2013;**2**(3): 246-279

[7] Colombo EF, Gialleonardo ED, Facchinetti A, Bruni S. Active car body roll control in railway vehicles using hydraulic actuation. Control Engineering Practice. 2014;**31**:24-34

[8] Gohrle C, Schindler A, Wagner A, Sawodny O. Design and vehicle implementation of preview active suspension controllers. IEEE Transactions on Control Systems Technology. 2014;**22**(3): 1135-1142

[9] Jin X-S, Xiao X-B, Ling L, Zhou L, Xiong J-Y. Study on safety boundary for high-speed trains running in severe environments. International Journal of Rail Transportation. 2013;**1**(1–2):87-108. DOI: 10.1080/23248378.2013.790138

[10] Nguyen SD, Choi SB, Nguyen QH. An optimal design of interval type-2 fuzzy logic system with various experiments including magnetorheological fluid damper. IMechE Part C: Journal of Mechanical Engineering Science. 2014;**228**(17): 3090-3106

[11] Nguyen SD, Nguyen QH. Design of active suspension controller for train cars based on sliding mode control, uncertainty observer and neuro-fuzzy system. Journal of Vibration and Control. 2017;**23**(8):1334-1353

[12] Kim HC, Choi SB, Lee GS. Performance analysis of a semi-active railway vehicle suspension featuring MR dampers. In: SPIE Smart Structures and Materials + Non-destructive Evaluation and Health Monitoring, San Diego, CA. Bellingham, WA: International Society for Optics and Photonics (SPIE); 2014. p. 905711

[13] Kumar PS, Sivakumar K, Kanagarajan R, Kuberan S. 2799 adaptive neuro fuzzy inference system control of active suspension system with actuator dynamics. Journal of Vibroengineering. 2018;**20**(1):541-549

[14] Matamoros-Sanchez AZ, Goodall RM. Novel mechatronic solutions incorporating inerters for railway vehicle vertical secondary suspensions. Vehicle System Dynamics. 2015;**53**(2): 13-136

[15] Oh J-S, Shin Y-J, Koo H-W, Kim H-C, Park J, Choi S-B. Vibration control of a semi-active railway vehicle

suspension with magneto-rheological dampers. Advances in Mechanical Engineering. 2016;**8**(4):1-13

[16] Suarez B, Felez J, Maroto J, Rodriguez P. Sensitivity analysis to assess the influence of the inertial properties of railway vehicle bodies on the vehicle's dynamic behaviour. Vehicle System Dynamics. 2013;**51**(2): 251-279

[17] Zolotas AG, Goodall RM. Modelling and control of railway vehicle suspensions. In: Turner MC, Bates DG, editors. Mathematical Methods for Robust and Nonlinear Control, Lecture Notes in Control and Information Sciences. New York: Springer; 2007. pp. 373-412

[18] Liang L, Xiao X-B, Xiong J-Y, Zhou L, Wen Z-F, Jin X-S. A three-dimensional model for coupling dynamics analysis of high speed train-track system. Journal of Zhejiang University Science A (Applied Physics and Engineering). 2014:1-21

[19] Sezer S, Atalay AE. Application of fuzzy logic based control algorithms on a railway vehicle considering random track irregularities. Journal of Vibration and Control. 2011;**18**(8):1177-1198

[20] Ulum Z, Affaf M, Salmah JCE, Suparwanto A. Active suspension systems design of a light rail vehicle using MPC with preview information disturbance. In: 5th International Conference on Instrumentation, Control, and Automation (ICA) Yogyakarta, Indonesia, August 9–11, 2017. pp. 18-23

[21] Sharma SK, Kumar A. Ride performance of a high-speed rail vehicle using controlled semi active suspension system. Smart Materials and Structures. 2017;**26**(1–19):055026